NANO LETTERS

2008
Vol. 8, No. 2
725−730

Polyelectrolyte Brush Amplified Electroactuation of Microcantilevers

Feng Zhou,[†] P. Maarten Biesheuvel,*[,†] Eun-Young Choi,[†] Wenmiao Shu,[†] Rosa Poetes,[‡] Ullrich Steiner,[‡] and Wilhelm T. S. Huck*[,†]

Melville Laboratory for Polymer Synthesis, University of Cambridge, Lensfield Road, Cambridge, CB2 1EW United Kingdom, and Department of Physics, Cavendish Laboratory, J. J. Thomson Avenue, Cambridge, CB3 0HE United Kingdom

Received December 4, 2007; Revised Manuscript Received January 11, 2008

ABSTRACT

This paper describes the electroactuation of microcantilevers coated on one side with cationic polyelectrolyte brushes. We observed very strong cantilever deflection by alternating the potential on the cantilever between +0.5 and −0.5 V at frequencies up to 0.25 Hz. The actuation resulted from significant increases in the expansive stresses in the polymer brush layer at both negative and positive potentials. However, the deflection at negative bias was significantly larger. We have developed a theoretical framework that correlates conformational changes of the polymer chains in the brush layer with the reorganization of ions due to the potential bias. The model predicts a strong increase in the polymer volume fraction, close to the interface, which results in large expansive stresses that bend the cantilever at negative potentials. The model also predicts that the actuation responds much stronger to negative potentials than positive potentials, as observed in the experiments.

Microcantilevers modified with self-assembled monolayers or polymeric coatings provide an ideal platform for the development of extremely sensitive chemical and biosensors.[1,2] Surface modification with DNA, proteins, or other organic molecules has been used to probe specific interactions in solution. These interactions induce conformational changes of the surface-bound materials leading to surface stresses that subsequently result in bending of the cantilevers.[3−5] It was recognized early on that these interactions, and in particular sequence-specific DNA hybridization, could be harnessed to provide the energy needed for nanoactuation.[6] In recent work, the folding of DNA structures on the surface of cantilevers has been used in nanomechanical studies.[7] However, although the actuation is robust, the building blocks used (proteins and DNA) are expensive and have limited availability. Electroactuation of cantilevers has been achieved using electroactive surface coatings, for example ferrocene-terminated monolayers, polyaniline (PAn), and polypyrrole (PPy).[8−10] In all these cases, electrochemical reactions occur during the potential sweep, resulting in solvation/desolvation of surface coatings and thus surface differential stresses. However, these coatings suffer either from low stress (ferrocene), and hence rather limited actuation in the case of monolayer-modified surfaces, or from delamination and structural deterioration with loss of redox behavior in physisorbed PAn and PPy films. As a result, stable and long-term actuation is rather difficult to achieve.

Here we report on the enhanced electroactuation of cantilevers modified with ultrathin polymer brushes chemically attached to one side of the cantilevers. The mechanism of actuation is not based on oxidation−reduction cycles but on the reversible perturbation of the electrical double layer associated with ion transport into and out of the polymer brush layer, as well as conformational changes of the grafted polymer chains. As described in detail below, electroactuation is due to changes in the structure of the brush phase directly near the electrified interface (within a few nm's). The balance of ion entropy and electrostatic energy in combination with chain elasticity (for the polymer segments) determine the equilibrium structure. Both at negative and positive applied voltages, the total ion concentration near the interface increases significantly, leading to an ion osmotic pressure contribution to the surface stress. In addition, electrostatic energy results in an expansive stress when the field strength is high near the cantilever, whereas at negative bias, the polycation brush segments form a very dense layer at the surface, which also exerts an expansive osmotic pressure, mainly due to volume constraints. We and others have demonstrated that polymer brushes can reversibly bend cantilevers due to conformational changes of the brush in response to changes in environmental conditions.[11−15] Although such schemes provide direct routes to the conversion of chemical energy into mechanical motion, changing pH, salt concentration, or temperature of the solution are slow

* To whom correspondence should be addressed. E-mail: mb668@cam.ac.uk; wtsh2@cam.ac.uk.
[†] Melville Laboratory.
[‡] Cavendish Laboratory.

10.1021/nl073157z CCC: $40.75
Published on Web 02/13/2008

Scheme 1. Cantilever Modified with Polyelectrolyte Brushes as Used in This Study and the Electroactuation Setup.

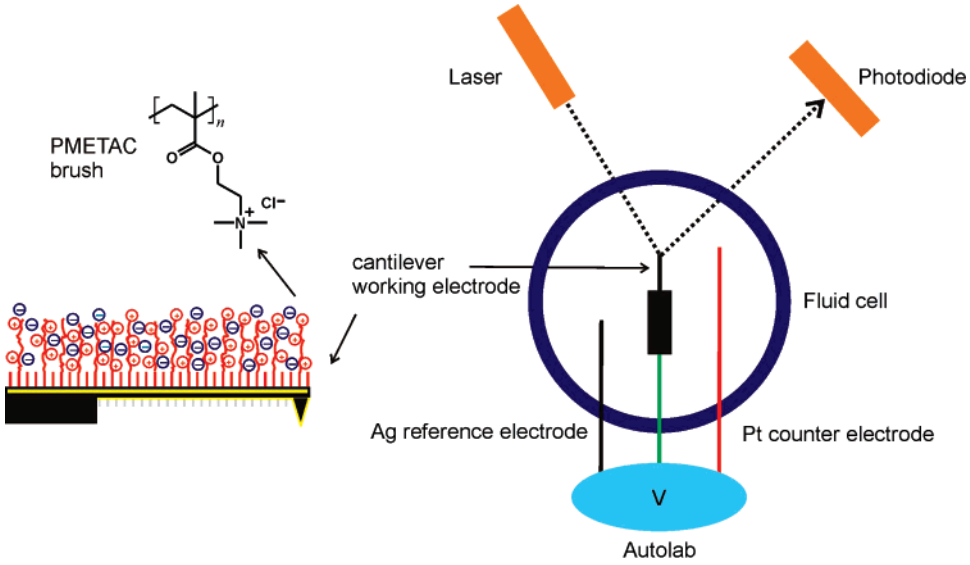

processes. Therefore, it will be extremely challenging to design "synthetic muscles" driven by oscillations in pH or salt concentration that exhibit high power densities.[16−17] External fields as used in this paper enable actuation without changes in solvent conditions and are therefore a promising route to fast, reversible actuation.

Poly[2-(methacrylolyloxy)ethyl] trimethyl ammonium chloride (PMETAC) brushes (45 nm dry thickness, as measured on reference surfaces) were grown from initiator-modified cantilevers (Veeco, V-shaped, length 220 μm, width 22 μm, thickness 600 nm, spring constant 0.03 N/m) as previously described.[14,18,19] The scanning frequencies in this work were all much below the resonance frequencies of the cantilevers in water of ∼3−4 kHz. Prior to the actuation experiments the force required to deflect the cantilever by a certain distance was estimated by measuring force distance curves for the gold plus brush-coated cantilevers. This "calibration" can be used to transform the actuation amplitude voltage (which is the signal obtained from the AFM) into a deflection in nm. Cantilever actuation was performed on a SPM 4500 system (Molecular Imaging) using a Teflon fluid cell containing a three electrode system with the Au film (cantilever), a Pt wire, and an Ag wire as working, counter and reference electrode, respectively (Scheme 1). The baseline drift of an oscillating cantilever system is common and has a number of causes (lack of temperature stability, piezo creep, etc.). Such drifts were observed irrespective of the cantilever details and cantilever actuation method (e.g., uncoated cantilevers that are actuated using the AFM's piezo show a similar drift). It is therefore common to normalize the cantilevers signal so that this drift is removed. Electrical control was obtained via an Autolab PGSTAT 30 system. Different electrolyte solutions were fully degassed by bubbling with N_2 for at least 2 h and the AFM chamber was kept under a N_2 atmosphere and at constant temperature during the actuation experiments. It should be noted that the growth of brushes on the cantilevers causes cantilever deflection. Therefore, all deflection vs time curves reported in this paper represent differential actuation, i.e., the difference in deflection between different applied values of bias. The magnitude of the deflection is on the order of 1 μm, which correlates with surface stresses on the order of 1 N/m.[14] Finally it should be noted that the experiments reported here were done using different cantilevers. Although the behavior was always the same, the magnitude of actuation differed between cantilevers. This is due to small differences between the different cantilevers in stiffness, thickness of the evaporated gold film, and the thickness of the brush layer.

In Figure 1a, sweeping potentials applied to the cantilever at a scanning rate of 100 mV/s from −0.5 to +0.5 V (i.e., 0.05 Hz, data acquisition time 1 s) in 1 mM $NaNO_3$ solution lead to highly reversible, very stable cantilever deflection. The figure also shows that polymer brush-coated cantilevers show very strong electroactuation compared to cantilevers coated with initiator monolayers. The frequency of actuation here is limited by the acquisition time in AFM setup. The cantilever deflection signal was found to be in-phase with the actuation bias, which can be explained by the fact that the scan rates were several orders of magnitude lower than all experimentally relevant time scales, such as time of ion diffusion across the brush layer and the resonance frequency of the cantilever in water.[20] Figure 1b shows that the magnitude of actuation remains stable for over 30 min (100 cycles).

A more detailed analysis of the deflection signal reveals that the deflection at −0.5 V is much greater than the deflection at +0.5 V. This asymmetry becomes clearer when plotting single actuation cycles of actuation experiments that were recorded with much shorter (200ms) acquisition times and different scan rates. Figure 1c,d shows actuation curves for different scan rates and at two different salt concentrations.

A number of observations can be made: the maximum cantilever deflection occurs at the most negative potential (−0.5 V). For the opposite potential of +0.5 V a smaller deflection in the same direction as for the negative potential

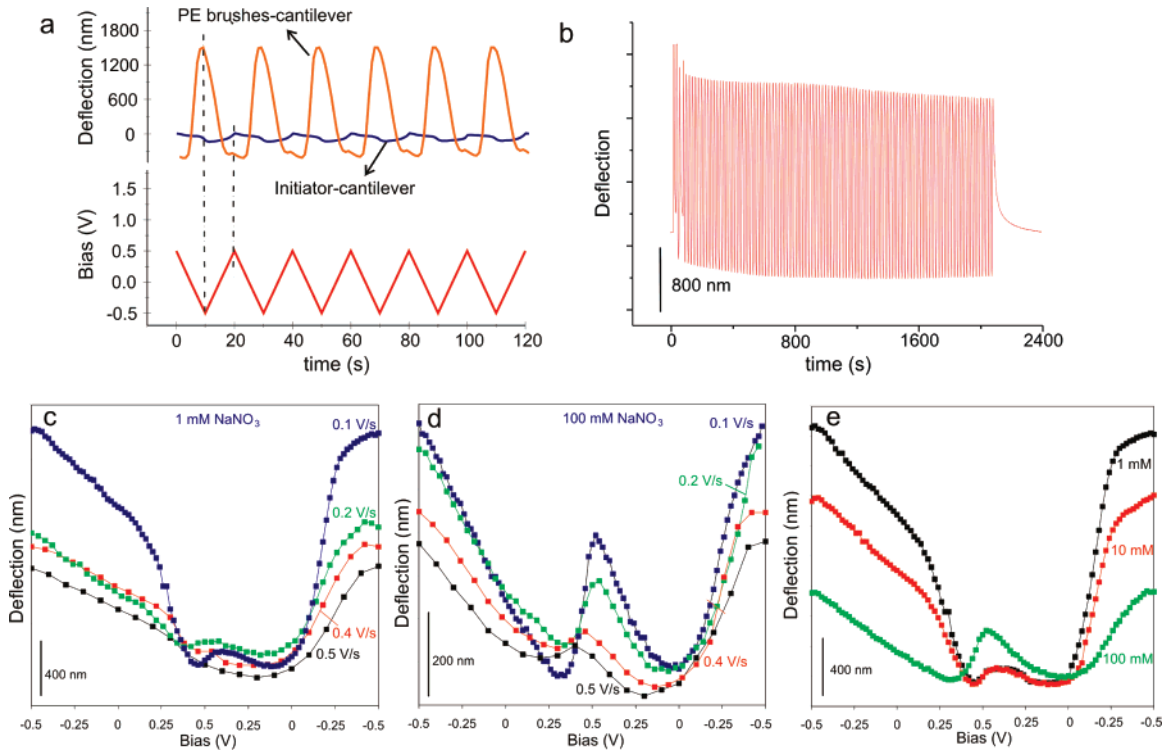

Figure 1. (a) Actuation of polymer brush-modified cantilever in response to the applied bias. The actuation directly follows the applied bias without apparent lag; initiator-only cantilevers show a very small response to changes in electric field. (b) Continuous actuation up to 100 cycles, showing a stable actuation amplitude, albeit with an overall drift in the signal. (c) and (d) Single cycle actuation traces at 1 mM and 100 mM $NaNO_3$ at different scanning rates. (e) Influence of salt concentration on deflection amplitude, scanning rate 0.1 V/s.

is observed. The minima in the deflection curve are, for many cases, not observed at 0 V, but in the bias range between +0.2 and +0.3 V. Note that the shape of the deflection curve of the downward sweep (from +0.5 to −0.5 V) and the upward sweep (from −0.5 to +0.5 V) differ. Different scanning rates have a strong influence on the actuation: faster scan rates lead to smaller deflection amplitudes, especially in the case of 1 mM electrolyte concentration, where the minimum deflection shifts toward 0 V. The high-salt deflection amplitude is considerably smaller than in the case of 1 mM salt. The effect of salt concentration on actuation is illustrated in more detail in Figure 1e, where single actuation cycles for 1, 10, and 100 mM salt concentrations are shown. Higher salt concentrations lead to a markedly smaller amplitude at −0.5 V, while the deflection at +0.5 V increases. The overall effect is a more symmetrical amplitude response to the downward and upward bias sweep. Such diminished responsiveness at increasing electrolyte concentrations can be correlated with increased charge screening effects in the polyelectrolyte brushes, which strongly affects the degree of chain stretching and hydration.[21−23]

The data presented here show the robust electroactuation of cantilever modified brushes, exhibiting a strong dependence on scanning potential, scan rates, and salt concentration. Our system is reminiscent of recent studies on conformational changes of surface-bound, strongly charged, single stranded DNA, where counterion distribution and orientation of the polymer chains is also seen to be strongly influenced by electric fields.[24−26] However, the polymer chains used in this study are significantly longer and more flexible, and the actuation observed here points to a much more complex responsive behavior. A full theoretical description of all of the characteristics observed above, especially dynamic effects such as the hysteresis between the upward and downward sweep and the considerable influence of the scan rate on the actuation amplitude, is beyond the scope of this manuscript. Here, we will present an approximate equilibrium model for the forces in the polymer brush and the resulting cantilever bending.

In equilibrium, the deflection D of a cantilever with thickness t and length L, covered on one side by a brush with height H (with $H \ll t$) is described, in the limit $D \ll L$, by a balance of torques, given by Stoney's equation[27]

$$\frac{t^2}{3L^2}\frac{E}{1-\nu^2}D = \frac{D}{\gamma} = \int_0^\infty \Pi \, dh \qquad (1)$$

where E is Young's modulus, ν is Poisson's ratio, and h is the height above the cantilever. The right-hand side of the equation represents the surface stress which is generated by the brush. It arises from the excess pressure Π (over that in solution) in the brush (or in the diffuse layer of ions extending from the top of the brush). The torque exerted by the diffuse layer of ions that is formed on the bottom side of the cantilever makes only a small contribution and is neglected.

The lateral pressure exerted on the cantilever includes contributions from the osmotic pressure of free ions (eq 2),

the interaction of brush segments (eq 3) and the electric field strength (eq 4):[28,29]

$$\Pi^{\text{ions}} = 2n_{\infty}(\cosh y - 1) \tag{2}$$

$$\Pi^{\text{brush}} = \frac{1}{\upsilon_b}\left(\phi^2 \frac{3-\phi^2}{(1-\phi)^3} - \upsilon\phi^2\right) \tag{3}$$

$$\Pi^{\text{lateral, field}} = \frac{\epsilon}{2}E^2 = \frac{n_{\infty}}{\kappa^2}\left(\frac{dy}{dh}\right)^2 = \frac{1}{8\pi\lambda_B}\left(\frac{dy}{dh}\right)^2 \tag{4}$$

where n_{∞} is the ionic strength (in nm^{-3}), y is the dimensionless electrostatic potential (voltage divided by the thermal voltage of 25.6 mV), υ_b is an empirical parameter, arising from the description of the polymer as a "chain-of-beads",[29] ϵ is the dielectric permittivity, κ is the inverse of the Debye length, and λ_B is the Bjerrum length. The first term in eq 3 describes excluded volume interactions between the polymer segments, and the second term is an attractive (e.g., hydrophobic) interaction. To simplify the calculation, we set $\upsilon = 3$, thereby imposing θ conditions; in this case, the dependence of Π^{brush} on ϕ^2 disappears, and thus excluded volume and attraction terms cancel in the dilute limit. While this simplifies eq 3, most uncharged polymers in water are better described by poor solvent conditions (i.e., $\upsilon \gg 3$).

To determine the lateral pressure Π by calculating the changes of ϕ and y with height, and thus to evaluate the lateral pressure, we used a modification of the so-called "box model" for polymer brushes.[28,29] A full analysis of the model and the assumptions made will be presented in a separate paper. In the box model, a force balance acting on the polymer chains is set up for each height h above the cantilever. The summation over all pressures Π (eqs 2−4), with a minus sign added to the contribution of the electric field given in eq 4 divided by grafting density σ, is equal to the elastic stretching force

$$f^{\text{elastic}} = \frac{3}{2}\frac{x}{k}\frac{2 - 4/5 \cdot x^2}{1 - x^2} \tag{5}$$

where k is the Kuhn length (a measure of the local chain stiffness) and $x = \sigma\upsilon_s/(a\phi)$ is the relative degree of stretching, stemming from the local brush volume fraction ϕ where υ_s is the volume per charged segment and a the distance (along the chain) between charged segments. Equation 5 is an extension of a Gaussian stretching model that includes finite-chain stretching. A more formal approach would use the complete Langevin equation, but for mathematical simplicity eq 5 is sufficiently accurate for our purpose. In a separate paper, we will compare different stretching models to describe the polymer density profile. To calculate electrostatic potentials, a modification of the Poisson−Boltzmann (PB) equation is used that includes the charges on the polymer and the fact that ions cannot penetrate the volume occupied by the polymer[30]

$$\frac{d^2y}{dh^2} = \kappa^2(1-\phi)\sinh y - 4\pi\lambda_B\frac{\phi}{\upsilon_s} \tag{6}$$

Furthermore, we include a charge-free Stern layer between the cantilever surface and the start of the brush phase ($y_{\text{cantilever}} - y_{\text{brush}}) = \delta_{St}\, dy/dh|_{h=0}$. We neglect any charge separation at the outer edge of the brush. Without an applied voltage, the PB equation simplifies to local electroneutrality and as a result the brush has the same volume fraction ϕ at each height, and x equals the dimensionless brush height H in terms of the contour length CL, $x = H/CL$. With an applied voltage, gradients develop in polymer density and potential near the cantilever. To calculate the brush height H we must evaluate the overall mass balance $\sigma N\upsilon_s = \int_0^H \phi\, dh$, where N is the number of charged segments per chain ($CL = Na$).

Figure 2a shows the calculated profiles of electrostatic potential in the brush, together with the volume fraction profiles for applied voltages of −0.5 and +0.5 V. For this calculation we used parameters based on the known dimensions of the cantilevers and estimated, but realistic, properties of the polymer brushes (grafting density, stiffness and length).[31] Interestingly, only a very thin region of 1−1.5 nm near the interface exhibits a change in the volume fraction, which is accompanied by a substantial potential variation. A positive applied voltage leads to a slight expansion of the brush near the cantilever surface where the potential is increased compared to the brush value of 0.2 V far from the surface. Note that there is a significant potential drop over the Stern layer of ∼0.15 V. However, in the case of a negative applied bias, we see a much larger influence of the applied voltage: the brush segments collapse onto the cantilever, increasing the volume fraction by 1 order of magnitude.

We now turn our attention to the question whether this rather localized change in density of the brush has an influence on the cantilever deflection. The calculation of the cantilever deflection can be carried out since we have the detailed profiles of the polymer volume fraction ϕ and electric field dy/dh inside the brush. We can therefore calculate the lateral pressure that, when integrated with respect to brush height, leads to the surface stresses that cause the cantilever bending (eq 1). The result of the calculation is shown in Figure 2b. Interestingly, the influence of the applied voltage is very large, especially at negative bias when the brush has formed a dense nanolayer at the cantilever interface. The calculation also predicts that the deflection at +0.5V is much smaller compared to the maximum deflection, in agreement with the experimental observations. The deflection vs voltage curve in Figure 2b shows the strikingly similar asymmetric actuation as the experimental results in Figure 1c−e, with absolute deflection minima on the downward sweep between 0.1 and 0.2 V. The simulated data show a similar trend in response to increased salt concentration, where the amplitude of actuation becomes smaller, but more symmetrical with a small increase in amplitude at +0.5 V and a significant decrease at −0.5 V.

The very good qualitative agreement between observed and predicted actuation is a strong indication that the

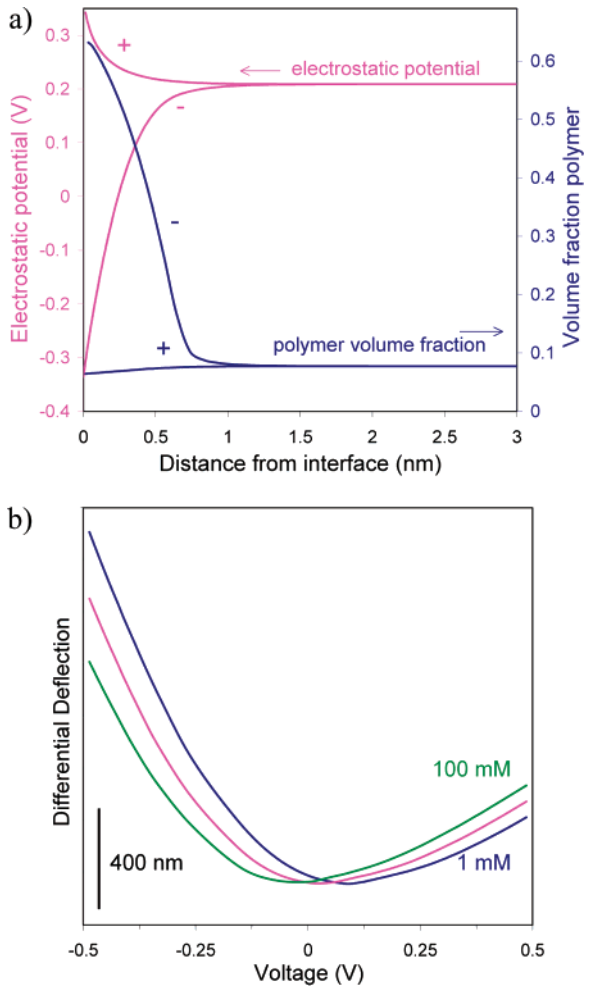

Figure 2. (a) Potential profile and polymer volume fraction in the polycationic brush near the cantilever at applied voltages of +0.5 and −0.5 V. (b) Predicted deflection as a function of applied voltage (bias) on the cantilever at different electrolyte concentrations.

mechanism for polyelectrolyte brush amplified electroactuation of cantilevers can be described in the following way: At −0.5 V, the charges on the positively charged polyelectrolyte chains are strongly attracted to the cantilever surface. As a result, the density of polymer chains near the surface increases markedly, generating a significant surface stress. The overall effect on the polymer brush layer is a reduction in brush thickness of around 5 nm. Cycling the potential to +0.5 V, pushes the polymer chains away from the surface, but draws negative counterions to the surface, again leading to additional surface stresses as when compared to the situation with no electric field bias.

While there is an excellent agreement between the experimental and theoretical curve shapes, not all aspects of the observed actuation cycle are described by the theory, which lacks a sufficiently detailed understanding of the dynamics of this system. To describe the hysteresis between upward and downward sweeps, a detailed analysis of dynamical aspects including the ion transport and polymer conformation changes is required, which will increase the level of complexity of the model calculation.

In conclusion, we have demonstrated how polyelectrolyte brushes can be used in the electroactuation of cantilevers. By applying an alternating positive and negative bias to a polyelectrolyte brush-covered cantilever, significant surface stresses are generated, which are several orders of magnitude larger compared to those obtained in DNA hybridization. Changing the sign of the applied bias did not reverse the direction of the deflection of the cantilever, but led to expansive stresses at the brush-covered side of the cantilever in both cases. We developed a theory based on a simplified polyelectrolyte brush model to describe the state of the brushes under positive and negative bias, and coupled this model to Stoney's equation for cantilever bending. This theory confirms that a bias in either direction should lead to expansive stresses, with stresses at negative potential which are significantly larger than for a positive bias. Our work opens new possibilities for studying the behavior of polymer brushes under electrical bias. In future work, we will explore the dynamics of the system in more detail, since preliminary results indicate that the cantilever actuation shows a complex time dependent response. The electroactuation demonstrated here has potential applications in microfluidic devices, where the ability to actuate without changing the chemical environment is strongly preferred.

Acknowledgment. We thank N.A.M. Besseling (TU Delft) for very useful discussions relating to the theory and the EPSRC (GR/T11555/01) for financial support.

References

(1) Yang, Y. M.; Ji, H. F.; Thundat, T. *J. Am. Chem. Soc.* **2003**, *125*, 1124.
(2) Zhang, J.; Lang, H. P.; Huber, F.; Bietsch, A.; Grange, W.; Certa, U.; McKendry, R.; Güntherodt, H. J.; Hegner, M.; Gerber, C. *Nat. Nanotechnol.* **2006**, *1*, 214.
(3) Berger, R.; Delamarche, E.; Lang, H. P.; Gerber, C.; Gimzewski, J. K.; Meyer, E.; Güntherod, H. J. *Science* **1997**, *276*, 2021.
(4) Burg, T. P.; Godin, M.; Knudsen, S. M.; Shen, W. J.; Carlson, G.; Foster, J. S.; Babcock, K.; Manalis, S. R. *Nature* **2007**, *446*, 1066.
(5) Wu, G.; Ji, H.; Hansen, K.; Thundat, T.; Datar, R.; Cote, R.; Hagan, M. F.; Chakraborty, A. K.; Majumdar, A. *Proc. Natl. Acad. Sci. U. S. A* **2001**, *98*, 1560.
(6) Fritz, J.; Baller, M. K.; Lang, H. P.; Rothuizen, H.; Vettiger, P.; Meyer, E.; Güntherodt, H. J.; Gerber, C.; Gimzewski, J. K. *Science* **2000**, *288*, 316.
(7) Shu, W.; Liu, D.; Watari, M.; Riener, C. K.; Strunz, T.; Welland, M. E.; Balasubramanian, S.; McKendry, R. *J. Am. Chem. Soc.* **2005**, *48*, 17054.
(8) Quist, F.; Tabard-Cossa, V.; Badia, A. *J. Phys. Chem. B* **2003**, *107*, 10691.
(9) Tabard-Cossa, V.; Godin, M.; Grütter, P.; Burgess, I.; Lennox, R. B. *J. Phys. Chem. B* **2005**, *109*, 17531.
(10) Lahav, M.; Durkan, C.; Gabai, R.; Katz, E.; Willner, I.; Welland, M. E. *Angew. Chem., Int. Ed.* **2001**, *40*, 4095.
(11) Bumbu, G. G.; Kircher, G.; Wolkenhauer, M.; Berger, R.; Gutmann, J. S. *Macromol. Chem. Phys.* **2004**, *205*, 1713.
(12) Bumbu, G. G.; Wolkenhauer, M.; Kircher, G.; Gutmann, J. S.; Berger, R. *Langmuir* **2007**, *23*, 2203.
(13) Abu-Lail, N. I.; Kaholek, M.; LaMattina, B.; Clark, R. L.; Zauscher, S. *Sens. Actuators B* **2006**, *114*, 371.
(14) Zhou, F.; Shu, W.; Welland, M. E.; Huck, W. T. S. *J. Am. Chem. Soc.* **2006**, *128*, 5326.
(15) Lemieux, M. C.; McConney, M. E.; Lin, Y. H.; Singamaneni, S.; Jiang, H.; Bunning, T. J.; Tsukruk, V. V. *Nano Lett.* **2006**, *6*, 730.
(16) Topham, P. D.; Howse, J. R.; Crook, C. J.; Armes, S. P.; Jones, R. A. L.; Ryan, A. J. *Macromolecules* **2007**, *40*, 4393.
(17) Howse, J. R.; Topham, P. D.; Crook, C. J.; Gleeson, A. J.; Bras, W.; Jones, R. A. L.; Ryan, A. J. *Nano Lett.* **2006**, *6*, 73.

(18) Jones, D. M.; Huck, W. T. S. *Adv. Mater.* **2001**, *13*, 1256.
(19) Cheng, N.; Azzaroni, O.; Moya, S.; Huck, W. T. S. *Macromol. Rapid Commun.* **2006**, *27*, 1632.
(20) Raiteri, R.; Butt, H. J. *J Phys. Chem.* **1995**, *99*, 15728.
(21) Moya, S.; Azzaroni, O.; Farhan, T.; Osborne, V. L.; Huck, W. T. S. *Angew. Chem., Int. Ed.* **2005**, *44*, 4578.
(22) Zhou, F.; Hu, H.; Yu, B.; Osborne, V. L.; Huck, W. T. S.; Liu, W. M. *Anal. Chem.* **2007**, *79*, 176.
(23) Biesalski, M.; Johannsman, D.; Ruehe, J.; *J. Chem. Phys.* **2004**, *120*, 8807.
(24) Rant, U.; Arinaga, K.; Fujuta, S.; Yokoyama, N.; Abstreiter, G.; Tornow, M. *Nano Lett.* **2004**, *4*, 2441.
(25) Rant, U.; Arinaga, K.; Fujuta, S. Yokoyama, N.; Abstreiter, G.; Tornow, M. *Org. Biomol. Chem.* **2006**, *4*, 3448.
(26) Shen, G.; Tercero, N.; Gaspar, M. A.; Varughese, B.; Shepard, K.; Levicky, R. *J. Am. Chem. Soc.* **2006**, *128*, 8427.
(27) Freund, L. B.; Suresh, S. *Thin Film Materials*; Cambridge University Press: Cambridge U.K., 2003.
(28) Biesheuvel, P. M. *J. Colloid Interface Sci.* **2004**, *275*, 97.
(29) Biesheuvel, P. M.; Leermakers, F. A. M.; Cohen Stuart, M. A. *Phys. Rev. E* **2006**, *73*, 011802.
(30) Biesheuvel, P. M.; van der Veen, M.; Norde, W. *J. Phys. Chem. B* **2005**, *109*, 4172.
(31) Parameter settings used in the calculation for Figure 2a,b: $\sigma = 0.4$ nm^{-2}, CL = 135 nm, $N = 540$, $a = 0.25$ nm, $\upsilon_s = 0.040$ nm^3, $\upsilon_b = 0.088$ nm^3, $k = 1$ nm, $\upsilon = 3$, $\lambda_B = 0.72$ nm. A cantilever geometry parameter, γ, is introduced in eq 1 for which we use $\gamma = 50$ nm^3/kT $= 12.1\ \mu$(m^2/N), $\delta_{St} = 0.345$ nm.

NL073157Z